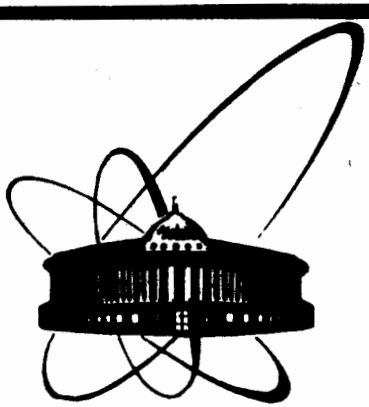

объединенный
институт
ядерных
исследований
дубна

E1-82-77

MUON PAIRS AND UPPER LIMIT FOR UPSILON PRODUCTION BY 280 GeV MUONS

BCDMS Collaboration

Submitted to "Nuclear Physics B"

1982

D.Bollini, P.L.Frabetti, G.Heiman, L.Monari, F.L.Navarria
Istituto di Fisica dell'Università and INFN, Bologna, Italy

A.C.Benvenuti[1], M.Bozzo[2], R.Brun, H.Gennow[3], M.Goossens,
R.Kopp, F.Navach, L.Piemontese, D.Schinzel
CERN, European Organization for Nuclear Research, Geneva,
Switzerland

S.P.Baranov[4], D.Yu.Bardin, N.D.Gagunashvili, I.A.Golutvin,
V.F.Grushin, Y.T.Kiryushin, A.A.Komar[4], V.G.Krivokhizhin,
V.V.Kukhtin, I.A.Savin, A.A.Shikanjan[4], M.G.Shafranova,
J.Strachota, A.G.Volodko, E.V.Telyukov[4]
JINR, Joint Institute for Nuclear Research, Dubna, USSR

D.Jamnik[5], U.Meyer-Berkhout, A.Staude, K.Teichert, R.Tirler,
R.Voss, Č.Zupančič
Sektion Physik der Universität, München, BRD[6]

J.Feltesse, J.Maillard, J.M.Malasoma, A.Milsztajn, J.F.Renardy,
Y.Sacquin, G.Smadja, P.Verrecchia, M.Virchaux
CEN, Saclay, France

1. INTRODUCTION

The production of muons in leptonic interactions with nucleons and nuclei is of particular interest in so far as some of these muons are the decay products of primarily produced heavy quarks (c,b,...)[1]. The toroidal spectrometer of the BCDMS Collaboration operating in the SPS muon beam at CERN has been designed to reach the large luminosity and the good acceptance for high p_T scattered muons necessary for the study of deep inelastic μ scattering at high Q^2. It is therefore also well suited for the study of muon pairs with large invariant mass.

2. EXPERIMENTAL SETUP AND DATA TAKING

The experimental apparatus is described in more detail elsewhere[2] and is schematically shown in fig.1. A carbon target ~40 m long, 12cm in diameter is centred in the 50 cm diameter bore of a segmented iron cylinder ~50 m long with 2.7 m external diameter. The magnetic field lines circle around the tar-

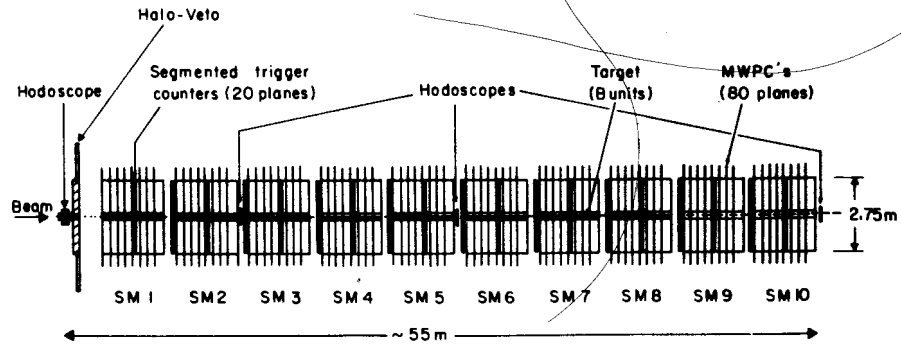

Fig.1. Schematic view of the experimental setup. Magnetized iron toroids with interspersed trigger counters and multiwire proportional chambers are arranged in ten supermodules (SM 1-10). The last two supermodules do not contain target units. A wall of scintillation counters vetoes the halo muons.

get, focusing positive and defocusing negative muons. Trigger counter and multiwire proportional chamber planes are placed at regular intervals perpendicular to the target (i.e., the axis of the cylinder) in the spaces between iron plates. The detector was triggered on tracks of sufficient length (~8 m or more) in time coincidence with an incident beam muon. The MWPC planes provided a scan of the tracks at ~1 m intervals in both orthogonal projections. After an automatic event preselection with very loose requirement, events containing more than one track were inspected on visual displays in order to eliminate spurious tracks.

The data were taken at the incident energy of 280 GeV with a total incident flux of $\sim 3\cdot10^{11}\mu^+$ corresponding to a total luminosity $L=(1.63\pm0.08)\cdot10^{39}cm^{-2}$. nucleon which yielded 629 $\mu^+\mu^-$ pairs. The number of equal sign muon pairs and trimuons was an order of magnitude smaller.

3. COMPARISON OF EXPERIMENTAL AND SIMULATED EVENTS

The most important sources of multimuons are the following:

i) π and K decays from hadronic showers produced in deep inelastic μ^+N scattering giving a detected μ^- in the spectrometer together with the scattered muon;

ii) direct muon pair production by the incident muon: $\mu^+N \to \mu^+\mu^+\mu^-X$ (QED tridents) with one μ^+ escaping detection through the central bore of the spectrometer;

iii) production and decay of hidden and open charm states (J/ψ, D, F, Λ_c, etc.). The detected muons are either both decay products or the positive one is the scattered muon while the negative one originates in the decay. About 95% of the observed open charm decay is of the second category.

Muons from these three sources were Monte-Carlo generated and traced through the apparatus in order to determine their relative contribution to the experimental sample.

The experimental distributions in multiplicity, energy and transverse momentum (with respect to the direction of the virtual photon) of mesons in hadronic showers were used to simulate multimuons induced by charged π and K decays [3].

QED tridents were generated [3,4] with weights equal to the differential cross-sections, as calculated from the diagrams of Fig.2 using the program SCHOONSCHIP [5]. Three production mechanisms were found to be important:

1) coherent production on the entire nucleus; the elastic carbon form factor was taken from Ref. [6];

2) quasi-elastic production on individual nucleons. The nucleon form factors with closure corrections were taken from Ref. [7], where the conventional description of quasi-elastic scattering was adjusted for the calculation of radiative corrections to eN scattering;

3) deep inelastic production on nucleons. The parametrization of nucleon structure functions was deduced from Refs. [7-10].

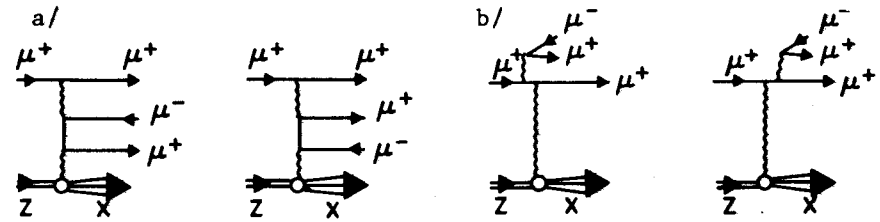

Fig.2. QED diagrams of $\mu^+\mu^-$ pair production: (a) Bethe-Heitler; (b) bremsstrahlung.

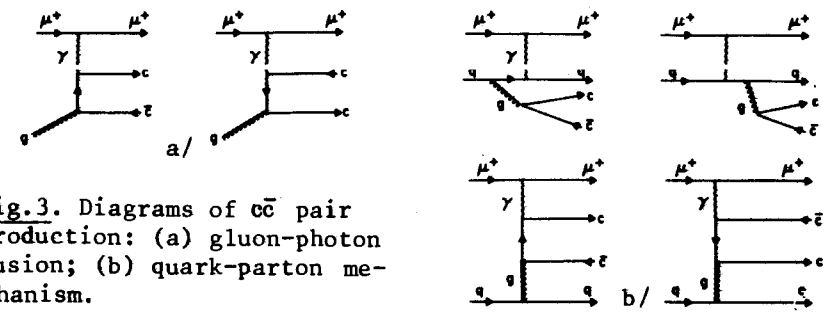

Fig.3. Diagrams of $c\bar{c}$ pair production: (a) gluon-photon fusion; (b) quark-parton mechanism.

The production of $c\bar{c}$ pairs was calculated [11], also by SCHOONSCHIP, from two sets of diagrams presented in Fig.3. The first set (a) represents the fusion of photons with "free" gluons in a nucleon. The second set (b) represents the fusion of photons with gluons emitted by quarks, i.e., the quark-parton mechanism of $c\bar{c}$ pair photoproduction. The latter set of diagrams yields contributions of the order α_{st}^2, i.e., about 10% of the usual free gluon-photon fusion cross-section.

The subsequent fate of $c\bar{c}$ pair was simulated in the following manner. If the invariant mass $M_{c\bar{c}}$ of the $c\bar{c}$ pair is larger than the J/ψ mass and smaller than twice the D° mass

(i.e., the open charm threshold), it was assumed that only the hidden charm states J/ψ and χ_J ($J^P=0^+, 1^+, 2^+$) can be produced with subsequent decays: $J/\psi \to \mu^+\mu^-$ and $\chi \to \gamma + (J/\psi \to \mu^+\mu^-)$. The relative production of J/ψ and χ states was set to 1:10, in agreement with the known cross-section for production of dimuons in the J/ψ region by incident muons [12,13]. For $M_{c\bar{c}}$ above the open charm threshold it was assumed that only the states D°, $D^\pm$, $F^\pm$ and Λ_c can be produced. The $c\bar{c}$ pair separates into two quarks, c and $\bar{c}$, which subsequently fragment independently according to the law $e^{-3.6z}$ with $z = E_h/E_q$, E_q and E_h being the energy of the quark and hadron in the $c\bar{c}$ pair center of mass system [14]. The priduction rates for D°, $D^\pm$, $F^\pm$, Λ_c were assumed in the ratio 2:1:1:1 as suggested by experimental data from e^+e^- collisions. Finally, the 3-body semileptonic decays of these charmed hadrons were simulated with the densities determined by matrix elements of Ref. [15]. The following branching ratios were assumed:

$$(D \to K\mu\nu) : (D \to K^*\mu\nu) : (D \to \pi\mu\nu) = 55 : 39 : 6,$$

$$(F \to \omega\mu\nu) : (F \to \phi\mu\nu) = (\Lambda_c \to \Lambda\mu\nu) : (\Lambda_c \to n\mu\nu) = 9 : 1.$$

The muons generated from the three sourced(i)-(iii)were traced through the experimental apparatus taking into account efficiencies in triggering and track reconstruction. In this way "effective" total cross-sections $\sigma_i^{eff} = \sigma_i \cdot \epsilon_i$ were determined, σ_i being the theoretical total cross-section for any of the processes (i)-(iii). The quantities ϵ_i are then the acceptance for dimuons from these processes. In an analogous manner and for each process separately, distributions in different kinematical quantities (e.g., energy of individual muon, invariant mass of the pair, etc.) were obtained. Some of the results are presented in Figs.4,5 and 6.

Figure 4 shows the distributions in the variables p_+ and p_- which are the momenta of the positive and negative muon, respectively. Figure 5 presents the distributions in the variables $p_{bal} = (p_+ - p_-)/(p_+ + p_-)$ and $p_T = |\vec{p}_+^{\,T} + \vec{p}_-^{\,T}|$, where $\vec{p}_+^{\,T}$ and $\vec{p}_-^{\,T}$ are the momenta of the positive and negative muon, respectively, transverse to the beam. Figure 6 shows the total spectrum of pair invariant masses M_{+-}. In these figures, the experimental histograms are confronted with absolute predictions for the different production mechanisms and for their sum.

We see that the qualitative features of all these distributions are well described by the simulation. The distributions in p_{bal} and p_T are rather sensitive to different production mechanisms and cuts on these variables can be used to enhance the contribution of a particular mechanism. Specifically we

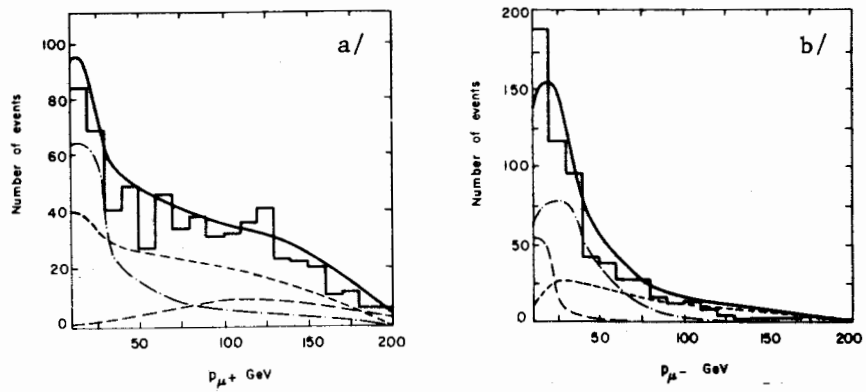

Fig.4. Momentum distributions: (a) p_+, (b) p_-. Histograms represent experimental data. Curves are contributions from Monte-Carlo simulated π,K decays (long dashed line), QED tridents (short dashed line), charmed particles (dashed-dotted line) and all together (solid line). The same convention is used in figs. 5,6 and 7.

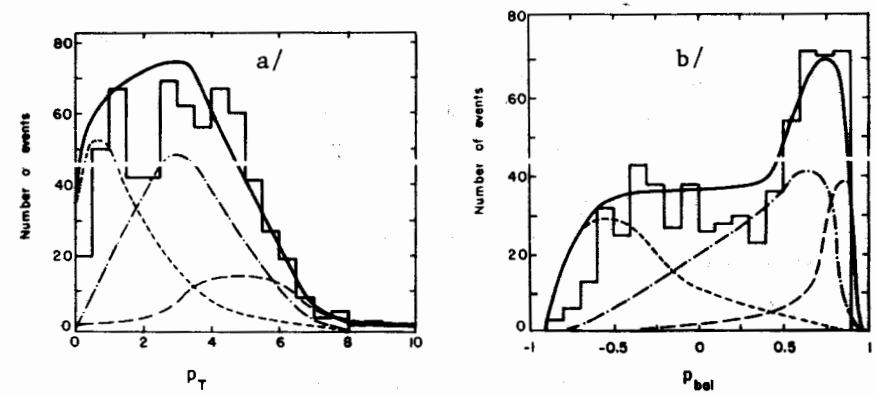

Fig.5. $\mu^+\mu^-$ pair distribution versus: (a) p_T, (b) p_{bal}.

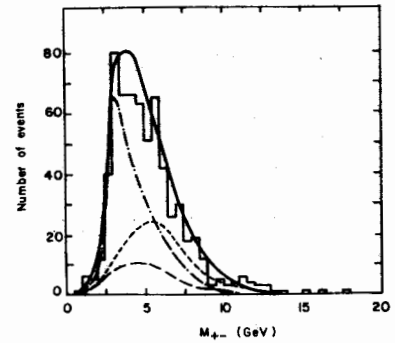

Fig.6. Distribution in pair invariant mass M_{+-}.

we use $p_T < 2$ GeV (symmetric pairs) to isolate a sample enriched in vector meson decays ($V \to \mu^+\mu^-$) while the remaining events (asymmetric pairs) originate primarily in open charm and π/K decays.

This cut is useful for investigating the small quantitative discrepancies apparent in Figs.4-6 and more succinctly presented in the Table. This Table observed number of events. While the agreement between data and prediction is good in case of asymmetric pairs, the number of predicted symmetric pairs exceeds the number of observed ones. Figure 7 shows the invariant mass spectrum of symmetric pairs. It is seen that the discrepancy between data and prediction is caused mainly by the invariant mass region below about 6 GeV, where the acceptance for symmetric pairs is low and fast varying.

Table

	Process	Prediction	Data
		N(events)	N(events)
Asymmetric pairs $P_T > 2$ GeV	π,K decay	85±8	
	QED tridents	67±10	
	Charm	295±21	
	TOTAL	447±24	451
Symmetric pairs $p_T < 2$ GeV	QED tridents	174±14	
	Charm	70±8	
	TOTAL	244±16	178
High mass Symmetric pairs $8 < M_{+-} \leq 12$ GeV $p_T < 2$ GeV	QED tridents	28.4±1.6	
	Charm	1.3±.5	
	TOTAL	29.7±1.7	27

4. UPPER LIMIT ON THE CROSS-SECTION FOR T PRODUCTION

The mass spectrum is shown in fig.7 for the events with $P_T < 2$ GeV. This cut reduces the contribution from T decays by only 5% while it eliminates most of the background contribution from the other processes. Since there is no direct evidence for the T we have considered the mass region $8\ \text{GeV} < M_{+-} \leq 12\ \text{GeV}$ to obtain an upper limit for T production. With the mass resolution better than 10% this requirement eliminated at most 2% of the T candidates. The Monte-Carlo simulation indicates that the events in this region are primarily from QED trident production, as is shown in the table.

Fig.7. Invariant mass distribution of symmetric pairs ($p_T < 2$ GeV) and the acceptance curve for vector particles decaying into $\mu^+\mu^-$ pairs (black points).

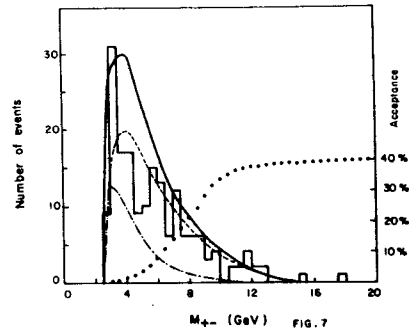

The absence of the T signal is confirmed also by fitting the mass continuum in control regions below 8 and above 12 GeV with a dependence M^{-a}. This fit gives $a = 2.45$ and 26.5 events in the T region as compared to 27 observed events. Therefore the upper limit at 90% confidence level on T production in this experiment was placed at 7 events as calculated from the statistical errors and the uncertainty in luminosity. With a detection efficiency $\epsilon_T = 0.32$ this corresponds to:

$$\sigma_T \cdot BR(T \to \mu^+\mu^-) < 13 \cdot 10^{-39}\ \text{cm}^2/\text{nucleon},$$

where σ_T is the T production cross-section for 280 GeV muons and $BR(T \to \mu^+\mu^-)$ is the branching ratio for $T \to \mu^+\mu^-$ decay. This limit is larger than the one quoted by us in 1979 as a preliminary result: $\sigma_T \cdot BR(T \to \mu^+\mu^-) < (6-9) \cdot 10^{-39}\ \text{cm}^2/\text{nucleon}$ [16] which was based on the analysis of another data set with different acceptance due to less restrictive trigger conditions. The difference between the two results is due more to our understanding of the processes involved in the Monte-Carlo simulation than to the data themselves.

The present estimate is to be compared to the upper limit of the BFP Collaboration [17], which is $48 \cdot 10^{-39}\ \text{cm}^2/\text{nucleon}$ when extrapolated to our beam energy. With $BR(T \to \mu^+\mu^-) = 3\%$ [18] the theoretical prediction [19] based on the photon gluon fusion model is $\sigma_T \cdot BR(T \to \mu^+\mu^-) = 12 \cdot 10^{-39}\ \text{cm}^2/\text{nucleon}$ for 280 GeV muons which does not contradict our upper limit.

REFERENCES

1. Glück M., Reya E. Phys.Lett., 1978, 79B, p.453; Leveille J.P., Weiler T. Nucl.Phys., 1979, B147, p.147; Brodsky S.J., Peterson C., Sakai N. SLAC-PUB-2660, 1981.
2. Bollini D. et al. Phys.Lett., 1981, 104B, p.403.
3. Brun R. et al. CERN DD/EE/78-1, June, 1980.
4. Akhundov A.A. et al. Jad.Fiz., 1980, 32, p.452.
5. Strubbe H. Comp.Phys.Com., 1974, 8, p.1.
6. Czyż W., Sheppev G.C., Walecka J.D. Nuovo Cim., 1964, 34, p.404.
7. Stein S. et al. Phys.Rev., 1975, D12, p.1884.
8. Brasse F.W. et al. Nucl.Phys., 1976, B110, p.413.
9. Anderson H.L. et al. Phys.Rev.Lett., 1976, 37, p.4; Gordon B.A. et al. Phys.Rev.Lett., 1978, 41, p.615; Gordon B.A. et al. Phys.Rev., 1979, D20, p.2645.
10. Bilen´kaya S.I., Khristova E.Kh. Jad.Fiz., 1978, 28, p.135.
11. Bardin D.Yu. et al. CERN/EP/NA-4 Note 81-23, 1981.
12. Clark A.R. et al. Phys.Rev.Lett., 1979, 43, p.187; 1980, 45, p.682.
13. Aubert J.J. et al. Phys.Lett., 1980, 94B, p.96,101.
14. Rapidis P.A. et al. Phys.Lett., 1979, 84B, p.507.
15. Barger V., Keung W.Y., Phillips R.J.N. Phys.Rev., 1979, D20, p.630.
16. Bollini D. et al. Proc. 1979 Int.Symp.on Lepton and Photon Interactions at High Energies (eds. T.B.W.Kirk and H.D.I.Abarbanel), p.149.
17. Clark A.R. et al. Phys.Rev.Lett., 1980, 45, p.686.
18. Schmidt-Parzefall W. Proc. XX Int.Conf.Madison (eds. L.Durand and L.G.Pondrom), p.692.
19. Fritzsch H., Streng K.-H. Phys.Lett., 1978, 72B, p.385.

Received by Publishing Department
on February 1 1982.

Боллини Д. и др. E1-82-77

Мюонные пары и верхний предел сечения генерирования T мюонами с энергией 280 МэВ

Изучались пары $\mu^+\mu^-$ с большой массой, генерированные μ^+ с энергией 280 ГэВ на углеродной мишени, с целью поиска T. Считается, что фон в интервале масс 2-18 ГэВ обязан КЭД парам, парам от распада очарованных частиц со скрытым и открытым чармом, а также парам, связанным с распадом адронов (π, K), образовавшихся в глубоконеупругих взаимодействиях. Верхний предел для сечения образования T мюонами на уровне 90% достоверности оказался: $\sigma_T \cdot BR(T \to \mu^+\mu^-) < 13 \cdot 10^{-39}$ см^2/нуклон.

Препринт Объединенного института ядерных исследований. Дубна 1982

Bollini D. et al. E1-82-77

Muon Pairs and Upper Limit for Upsilon Production by 280 GeV Muons

The high mass $\mu^+\mu^-$ pairs produced by 280 GeV μ^+ on a carbon target are studied in a search for the T production. The high mass continuum in the region 2-18 GeV is interpreted in terms of QED pair production and of μ pairs originating from the decay of hidden and open charm particles as well as of hadrons (π, K) from deep inelastic interactions. The upper limit for the upsilon production by muons is found to be at the 90% confidence level: $\sigma_T \cdot BR(T \to \mu^+\mu^-) < 13 \cdot 10^{-39}$ cm^2/nucleon.

Preprint of the Joint Institute for Nuclear Research. Dubna 1982